Neurobiology of Aging 79 (2019) 59–65

Contents lists available at ScienceDirect

Neurobiology of Aging

journal homepage: www.elsevier.com/locate/neuaging

Quantitative assessment of the intracranial vasculature in an older adult population using iCafe

Li Chen [a], Jie Sun [b], Daniel S. Hippe [b], Niranjan Balu [b], Quan Yuan [c], Isabelle Yuan [d], Xihai Zhao [e], Rui Li [e], Le He [e], Thomas S. Hatsukami [f], Jenq-Neng Hwang [a], Chun Yuan [b,*]

[a] Department of Electrical Engineering, University of Washington, Seattle, WA, USA
[b] Department of Radiology, University of Washington, Seattle, WA, USA
[c] Department of Neurology, Xuanwu hospital, Capital Medical University, Beijing, China
[d] Wellesley College, Wellesley, MA, USA
[e] Biomedical Engineering, Tsinghua University, Beijing, China
[f] Department of Surgery, University of Washington, Seattle, WA, USA

ARTICLE INFO

Article history:
Received 22 October 2018
Received in revised form 4 February 2019
Accepted 28 February 2019
Available online 28 March 2019

Keywords:
iCafe
Aging
Vascular change
Feature extraction
Intracranial artery
Vascular biomarker

ABSTRACT

Comprehensive quantification of intracranial artery features may help us assess and understand variations of blood supply during brain development and aging. We analyzed vasculature features of 163 participants (age 56–85 years, mean of 71) from a community study to investigate if any of the features varied with age. Three-dimensional time-of-flight magnetic resonance angiography images of these participants were processed in IntraCranial artery feature extraction technique (a recently developed technique to obtain quantitative features of arteries) to divide intracranial vasculatures into anatomical segments and generate 8 morphometry and intensity features for each segment. Overall, increase in age was found negatively associated with number of branches and average order of intracranial arteries while positively associated with tortuosity, which remained after adjusting for cardiovascular risk factors. The associations with number of branches and average order were consistently found between 3 main intracranial artery regions, whereas the association with tortuosity appeared to be present only in middle cerebral artery/distal arteries. The combination of time-of-flight magnetic resonance angiography and IntraCranial artery feature extraction technique may provide an effective way to study vascular conditions and changes in the aging brain.

1. Introduction

Older age is a major risk factor for cardiovascular disease and is associated with a number of deleterious changes in the cardiovascular system, such as coronary disease, hypertension, congestive heart failure, and stroke (Lakatta and Levy, 2003; Najjar et al., 2005). Age-specific mortality rates from heart disease and stroke increase exponentially with age throughout the later years of life, accounting for more than 40% of all deaths among people aged 65–74 years and almost 60% at age 85 years and older (Ungvari et al., 2010).

Various vascular changes with normal aging have been explored, especially in the older adult population. Previous studies have identified microvascular and macrovascular changes associated with aging, including decreased microvascular density (Brown and Thore, 2011), loss of microvascular plasticity (Riddle et al., 2003), progressive luminal dilation (Gutierrez et al., 2016), increased vessel tortuosity (Kamenskiy et al., 2015), and vessel wall thickening (Farkas et al., 2006). In addition to arterial structural changes, unsurprisingly, aging has also been shown to lead to significant changes in cerebral vascular flow (Kalaria, 1996; Kety, 1955; Scheinberg et al., 1953). Quantifiable from three-dimensional time-of-flight (TOF) magnetic resonance angiography (MRA) (Bullitt et al., 2003, 2009; Wright et al., 2013), brain arterial maps can be generated to reflect the vascular supply of the brain (Bernier et al., 2018; Viviani, 2016), and these physiological and pathophysiological changes in cerebral vasculature are believed to be implicated in the pathogenesis of many common neurological diseases such as stroke and Alzheimer's disease (Arvanitakis et al., 2016; Webster et al., 1995; Yonas et al., 1993).

However, the lack of appropriate quantitative image analysis tools and insufficient data limit studies of cerebral vascular flow and

* Corresponding author at: Department of Radiology, University of Washington, Box 358050 850 Republican St, Rm 127, Seattle, WA, 98109-4714. Tel.: +1 206-543-3061; fax: +1 206-616-9354.
E-mail address: cyuan@uw.edu (C. Yuan).

0197-4580/$ – see front matter © 2019 Elsevier Inc. All rights reserved.
https://doi.org/10.1016/j.neurobiolaging.2019.02.027

structure changes in the older adults. Most processing techniques are limited to simple structural characterization (number, average radius, and tortuosity) of only a portion of the cerebral arterial tree, thus may miss some global and regional changes in intracranial vasculature. Comprehensive TOF MRA analysis may detect subtle regional vascular changes with aging but has not yet been performed in a large cohort of older adult population. Thus, a comprehensive analysis approach that can quantify vascular features at both global and subregional levels is needed to better understand these relationships between the vascular changes and aging.

Intra**C**ranial **a**rtery **f**eature **e**xtraction technique (iCafe) (Chen et al., 2018a,b) is a recently developed and validated technique that can evaluate morphometry and intensity features of all vascular regions identified in the brain from TOF MRA images. A reproducibility evaluation of iCafe demonstrated that intracranial artery features quantified by iCafe had good to excellent interscan and intraoperator/interoperator reproducibility (Chen et al., 2018b). With this semiautomated analysis method, each visible artery can be digitally reconstructed with centerline, radius, intensity and artery name available, providing an opportunity to quantify structural and flow-related changes in each possible vasculature territory.

In this study, we used iCafe to comprehensively quantify intracranial vascular features in a cohort of 163 older adults from a community in China to explore their relationships with aging.

2. Methods

2.1. Study population

Three-dimensional TOF MRA of 163 participants (age 56–85 years old, mean and standard deviation of 71.6±5.9 years, 74 males) from a pilot community study in China, Cardiovascular Risk of Older Population (Cai et al., 2017; Han et al., 2018; Huang et al., 2017; Huang et al., 2016; Huang et al., 2017; Jiang et al., 2015; Qiao et al., 2016; Zhou et al., 2016), was analyzed. All participants with intracranial TOF MRA and clinical information available were selected for analysis from this study. No participants were excluded because of inadequate image quality in TOF MRA. The inclusion criteria for the Cardiovascular Risk of Older Population study were as follows: (1) enrollment was open to all retirees in the community of Tsinghua University; (2) participants had no cardiovascular symptoms within 6 months before MR imaging. Participants who had contraindications to MR imaging were excluded from this study. The study followed local institutional review board guidelines, and informed consent was obtained for all participants before enrollment.

Three-dimensional TOF images were scanned on a 3.0 T Philips MR scanners (Achieva TX, Best, the Netherlands). Imaging parameters of TOF MRA were as follows: repetition time/echo time = 25/3.5 ms, flip angle = 20°, in-plane resolution = 0.35 mm × 0.35 mm, slice thickness = 1.4 mm, field of view = 180 mm × 180 mm × 84 mm. Owing to restrictions on scan time, isotropic whole-brain scans were not performed for this study. The TOF field of view was centered on the major vessels.

2.2. Feature extraction

All the MRA images were processed using iCafe (Chen et al., 2018a). Briefly, the procedure of iCafe processing includes the following steps. MRA images were resampled into isotropic-sized voxels of 0.35 mm^3 in three-dimensional space, and image intensities were normalized using the Nyul (Nyul et al., 2000) method to allow comparable intensity features from different participants in the data set. Artery regions in images were segmented using a deep learning approach (Chen et al., 2017a,b), then artery regions were traced using an improved open-curve active contour model (Wang et al., 2011), and manual corrections to the traces were made as needed so that arteries in the original MRA image were reconstructed into a network of radius varying tubular structures with known centerline positions. Arteries were then labeled using a maximum a posteriori model as 1 of the 24 artery types defined in iCafe (Fig. 1). The images were analyzed by a neurologist with 20 years of experience and the iCafe developer who revised cases until consensus was reached. Images were reviewed in random order and blinded to age and other clinical information.

2.3. Available vascular features

The analysis focused on the vascular features of the bilateral anterior cerebral arteries (ACAs), middle cerebral arteries (MCAs), and posterior cerebral arteries (PCAs). For the primary analysis, the features were calculated over all arteries together (ACAs, MCAs, and PCAs). Further subanalyses were performed on the vascular features calculated separately for different territories: left and right; proximal (A1, M1, and P1 segments), and distal (A2+, M2+, and P2+ segments); ACAs, MCAs, and PCAs; and M1, M2, M3+ segments.

A total of 7 morphometry features and 1 intensity feature were defined and computed for each artery and artery group analyzed in this study. Good to excellent reproducibility of these features has been previously reported (Chen et al., 2018b).

2.3.1. Morphometry features

Number of branches is the number of traces which start from a bifurcation and end in another bifurcation or termination in a vascular group. Artery length is the end-to-end distance of the centerline of an artery or artery group. Average artery diameter is the average diameter along the centerline of each artery. Artery volume is the total volume in the reconstructed artery or artery group. Tortuosity is the ratio between artery length and the Euclidean distance of the 2 terminal points of an individual artery segment. For a vascular group, the tortuosity values of the constituent arteries were averaged. The artery bifurcation angle of an artery segment is the minimum angle at the bifurcation point. If the branch has bifurcations at both ends, the mean of 2 minimum angles is taken. For a vascular group, the bifurcation angle values of the constituent arteries were averaged. The order of an artery is defined as the number of branches on the minimum path from that artery to an internal carotid artery for anterior arteries or the basilar artery for posterior arteries.

2.3.2. Intensity feature

Average normalized intensity is the average intensity of the centerline points in an artery or vascular group after intensity normalization by the Nyul (Nyul et al., 2000) method.

2.4. Statistical analysis

The primary analysis was to examine the association of each overall vascular feature (calculated from all the arteries together) with age, adjusted for sex, using the partial Pearson correlation coefficient. There were 8 vascular features, so multiple hypothesis testing was accounted for by using Holm's method to assess statistical significance. In Holm's method, the smallest p-value is compared to 0.00625 (0.05 divided 8), similar to the Bonferroni correction. However, the other p-values have less strict significance thresholds, so Holm's method is less conservative than Bonferroni's.

Secondary analyses included correlating age with vascular features of subterritories as defined in the previous section, comparing

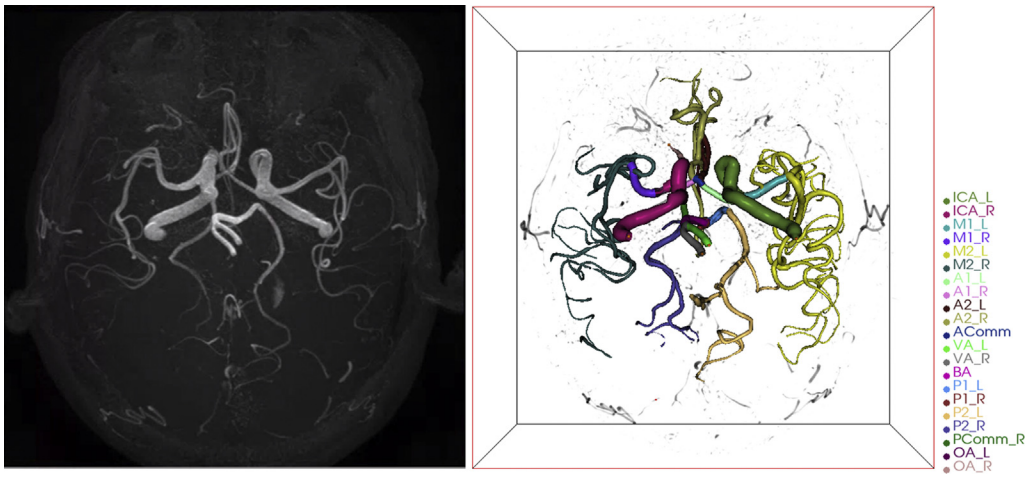

Fig. 1. Maximum intensity projection of original 3D TOF MRA image (left) and 3D visualization (right) of traced arteries in iCafe [artery definition in (Chen et al., 2018a)]. Abbreviations: 3D, three-dimensional; TOF, time-of-flight; MRA, magnetic resonance angiography.

correlation coefficients between subterritories using the nonparametric bootstrap, and further adjusting correlations with age by traditional cardiovascular risk factors (summarized in Table 1) and an imaging biomarker of large-artery disease, mean carotid vessel wall thickness. Carotid vessel wall thickness was evaluated in a previous study of this cohort (Cai et al., 2017) and as a novel imaging biomarker may reflect the cumulative effect of cardiovascular risk factors. These additional correlation adjustments were performed to test the hypothesis that age is associated with the vascular features independent of cardiovascular comorbidities which tend to increase in prevalence with age.

Holm's multiple comparison adjustment was applied to each secondary subanalysis separately rather than to all of them at once to control the false-positive rate while still retaining reasonable statistical power. For example, when analyzing the partial correlation of vascular features of the ACA, MCA, and PCA separately, which involved 24 tests (8 features × 3 territories), Holm's method was applied to those 24 tests (worst-case significance threshold of 0.0021).

R (version 3.1.1) was used for all statistical analyses.

3. Results

The clinical characteristics of the study cohort are shown in Table 1. More than half were female (55%). Age ranged from 56 to 85 years (median: 71 years). Cardiovascular risk factors were common, with the Framingham 10-year cardiovascular risk score ≥20% in 40% of the study cohort. Vascular features are summarized in Table 2 for all arteries and separate territories of interest.

The associations between overall vascular features and age are shown in Table 3 and Fig. 2. Aggregated across all arteries, the number of branches (partial r = −0.38), average order (partial r = −0.39), and average tortuosity (partial r = 0.27) were significantly associated with age after adjusting for sex and accounting for the number of tests.

The number of branches, average order, and average tortuosity were not associated with any individual cardiovascular risk factors in Table 1 (data not shown). Their associations with age remained statistically significant after further adjusting for traditional cardiovascular risk factors or mean carotid vessel wall thickness (Table 3), except for average tortuosity, which showed a borderline association with age after adjusting for traditional cardiovascular risk factors.

As the overall aggregated vascular features were associated with age, we further explored several vascular subgroups and whether their association with age differed. The vascular features of the left and right territories had similar associations with age as the overall features, without any statistically significant differences between left and right (data not shown). For the proximal arteries, average tortuosity did not appear to be associated with age (partial r = −0.06, 95% CI: −21, 0.10, $p = 0.47$). However, tortuosity of the distal arteries was associated with age (partial r = 0.28, 95% CI: 0.15, 0.40, $p < 0.001$) with the difference between proximal and distal arteries being statistically significant after accounting for the number of features compared ($p = 0.001$).

The number of branches and average order of the ACA, MCA, and PCA arteries each had similar associations with age with partial correlation coefficients ranging from −0.26 to −0.32 ($p \leq 0.001$ for all) with no significant differences between the territories (Table 4 and Fig. 3). By contrast, average tortuosity was more significantly

Table 1
Clinical characteristics of the study participants

Variable	No. (%) or median (Range)
Male sex	74 (45.4)
Age, years	71 (56–85)
Body mass index, kg/m2	24 (15–34)
History of hypertension[a]	80 (49.4)
Hypertension medication[a]	78 (48.8)
History of hyperlipidemia[a]	105 (64.8)
History of diabetes[a]	30 (18.5)
Smoking history[a]	
Never	141 (87.0)
Former	15 (9.3)
Current	6 (3.7)
Systolic blood pressure[a], mg Hg	130 (96–180)
Diastolic blood pressure[a], mg Hg	71 (49–100)
Total cholesterol[a], mg/dL	187 (117–310)
LDL-C, mg/dL	112 (49–206)
HDL-C, mg/dL	55 (28–113)
Triglycerides, mg/dL	108 (40–695)
Framingham risk score for 10-y CVD[a], %	
Low risk (<10%)	42 (27.3)
Intermediate risk (10%–20%)	51 (33.1)
High risk (≥20%)	61 (39.6)

Key: CVD, cardiovascular disease; HDL-C, high-density lipoprotein cholesterol; LDL-C, low-density lipoprotein cholesterol.

[a] Participants with missing values were excluded from the corresponding summary: history of hypertension (n = 1), hypertension medication (n = 3), hyperlipidemia (n = 1), diabetes (n = 1), blood pressure (n = 4), lipids (n = 6), and Framingham risk score for 10-y CVD (n = 9).

Table 2
Associations between age and vascular features derived from all arteries

Variable	All	Side		Location		Major territory		
	Arteries	Left	Right	Proximal	Distal	ACA	MCA	PCA
Total length, cm	313 ± 48	154 ± 27	158 ± 27	10 ± 1	302 ± 47	43 ± 12	211 ± 35	59 ± 15
Average diameter, mm	1.4 ± 0.1	1.5 ± 0.1	1.4 ± 0.1	3.2 ± 0.3	1.4 ± 0.1	1.8 ± 0.2	1.3 ± 0.1	1.8 ± 0.2
Volume, cm^3	6.8 ± 1.2	3.4 ± 0.6	3.4 ± 0.7	0.9 ± 0.2	5.9 ± 1.1	1.3 ± 0.4	3.7 ± 0.7	1.8 ± 0.6
Number of branches	134 ± 26	66 ± 15	68 ± 15	6 ± 0	128 ± 26	22 ± 7	84 ± 17	29 ± 10
Average order	5.1 ± 0.4	5.0 ± 0.5	5.1 ± 0.4	2.0 ± 0.0	5.2 ± 0.4	4.9 ± 0.7	4.9 ± 0.3	5.4 ± 0.9
Average tortuosity	1.7 ± 0.1	1.7 ± 0.1	1.7 ± 0.2	1.2 ± 0.1	1.7 ± 0.1	1.4 ± 0.1	1.8 ± 0.1	1.5 ± 0.1
Average bifurcation angle, degrees	56 ± 5	56 ± 7	56 ± 6	58 ± 15	56 ± 5	61 ± 9	53 ± 6	64 ± 9
Average normalized intensity	119 ± 14	120 ± 15	118 ± 14	253 ± 40	114 ± 13	151 ± 23	108 ± 14	136 ± 15

Values are mean ± SD; all arteries = ACA, MCA, PCA; left = left ACA, MCA, PCA; right = right ACA, MCA, PCA; proximal = A1, M1, P1; distal = A2+, M2, M3+, P2+; ACA = A1, A2+; MCA = M1, M2, M3+; PCA = P1, P2+.
Key: ACA, anterior cerebral artery; MCA, middle cerebral artery; PCA, posterior cerebral artery.

associated with age in the MCA territory (partial r = 0.30, $p < 0.001$) than in the other 2 territories (partial r from −0.02 to 0.02). The association between age and tortuosity was similar in the M2 (partial r = 0.17, 95% CI: 0.01, 0.31, $p = 0.033$) and M3+ territories (partial r = 0.26, 95% CI: 0.12, 0.39, $p = 0.001$) without a significant difference between them ($p = 0.39$).

4. Discussion

In this cross-sectional study, complete intracranial arterial maps were reconstructed, and comprehensive vascular features were extracted using a novel intracranial artery tracing and feature extraction technique. With this comprehensive feature extraction tool, we found that increase in age was associated with fewer branches, a lower average order, and higher tortuosity in the intracranial vasculature. The relationships of age with number of branch and average order were found in all 3 major territories while age appeared to be correlated with tortuosity in the MCA territory but not in the ACA or PCA territory. Most of these associations remained statistically significant after further adjustments for potential effects by cardiovascular risk factors, indicating an independent effect of age on the intracranial artery features.

4.1. Accurate and comprehensive description of the intracranial vasculature

The accuracy and reproducibility of iCafe-extracted vascular features are critical for the technique to be applied to evaluate individual variations in clinical studies. As manual segmentation of all intracranial arteries as a gold standard is not realistic, iCafe-extracted vascular features have been previously validated by comparing stenosis and bifurcation identification as well as artery length measurement by iCafe to manual results (Chen et al., 2018a). In addition, its interscan and intraoperator/interoperator reproducibility have been evaluated recently (Chen et al., 2018b). The present study is the first clinical study in which iCafe was used to understand physiological and pathophysiological changes in the intracranial vasculature. With comprehensive analysis of intracranial arteries using iCafe, the intracranial arteries can be divided into user-defined groups, so that both regional and global features can be analyzed.

We found that there was an age-related decrease of the number of branches (average order), but not across right/left brain or across flow territories (MCA/ACA/PCA). This finding suggests the underlying mechanisms leading to attenuation of arteries with aging are systemic. On the other hand, there was a clear difference of average tortuosity of artery changes in distal and proximal groups and within flow territories, suggesting that the vascular tortuosity alterations are more likely in distal small arteries than proximal large branches. With these findings, we not only confirmed the change of intracranial arteries through aging but also made a step further to pinpoint the location of these changes, which may help to gain better understanding of mechanisms of normal aging and the pathophysiology of intracranial arterial deterioration with aging.

Features such as artery number and branch order measured in our study using angiography are reflective of blood flow to the brain. Visibility of arteries and hence more branches or higher branch order indicates that blood supply is present to those brain regions distal to the visible arteries. For distal arteries, which are naturally smaller in radius and slower in flow velocity, the visibility on TOF due to reduced flow is more sensitive than proximal branches. Thus absence (i.e., nonvisibility) of arteries suggests that blood supply may be reduced to distal brain regions.

Table 3
Associations between age and vascular features derived from all arteries after adjustments

Variable	Adjusted only for sex[a] (N = 163)			Adjusted for sex and traditional risk factors[b] (N = 155)			Adjusted for sex and mean carotid wall thickness[c] (N = 140)		
	Partial r[a]	(95% CI)	*p*-value	Partial r[b]	(95% CI)	*p*-value	Partial r[c]	(95% CI)	*p*-value
Total length	−0.18	(−0.31, −0.04)	0.021	−0.16	(−0.29, −0.02)	0.059	−0.17	(−0.31, −0.03)	0.047
Average diameter	0.02	(−0.13, 0.17)	0.80	0.08	(−0.08, 0.25)	0.36	0.07	(−0.10, 0.23)	0.41
Volume	−0.14	(−0.27, −0.00)	0.074	−0.08	(−0.22, 0.08)	0.35	−0.11	(−0.25, 0.04)	0.20
Number of branches	**−0.38**	**(−0.49, −0.26)**	**<0.001**[d]	**−0.34**	**(−0.47, −0.21)**	**<0.001**[d]	**−0.38**	**(−0.50, −0.25)**	**<0.001**[d]
Average order	**−0.39**	**(−0.50, −0.27)**	**<0.001**[d]	**−0.35**	**(−0.48, −0.21)**	**<0.001**[d]	**−0.35**	**(−0.48, −0.22)**	**<0.001**[d]
Average tortuosity	**0.27**	**(0.14, 0.40)**	**<0.001**[d]	0.16	(0.02, 0.30)	0.056	**0.28**	**(0.13, 0.41)**	**0.001**[d]
Average bifurcation angle	−0.08	(−0.24, 0.07)	0.28	−0.15	(−0.30, 0.00)	0.078	−0.06	(−0.23, 0.10)	0.46
Average normalized intensity	0.01	(−0.13, 0.16)	0.86	0.04	(−0.14, 0.19)	0.62	0.07	(−0.10, 0.23)	0.44

Significant relations are given in bold.
[a] The partial Pearson correlation coefficient between the vascular feature and age, adjusted for sex.
[b] The partial Pearson correlation coefficient between the vascular feature and age was adjusted for sex, BMI, hypertension, hyperlipidemia, diabetes, smoking history, blood pressure, LDL-C, HDL-C, and triglycerides in participants with complete clinical data.
[c] The partial Pearson correlation coefficient between the vascular feature and age was adjusted for sex and mean carotid vessel wall thickness in participants with carotid wall thickness measurements.
[d] Statistically significant after accounting for the number of comparisons per model (Holm's method).

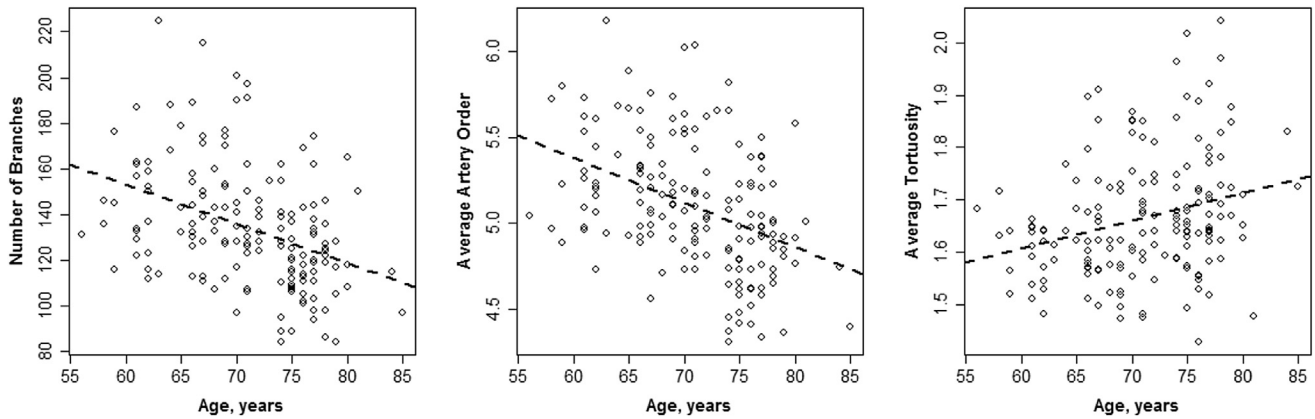

Fig. 2. Scatterplots of the overall vascular features significantly associated with age as shown in Table 3. The least squares fit lines are indicated by the dashed lines.

The increase of average artery tortuosity for MCA but not ACA or PCA may need further investigation from the perspective of brain atrophy in different regions (Raz et al., 2005; Scahill et al., 2003).

In addition to these flow-related structural features reflected from morphometry, we also explored the artery flow–related information using normalized signal intensity of arteries. However, none of these features showed statistically significant correlations with age. This suggests that flow-related morphometry changes may be more dominant than flow velocity–related intensity changes of intracranial arteries with aging.

4.2. Related previous studies

Previous studies focused on a limited number of intracranial artery regions using a small number of vascular features. Zurada et al., 2011, 2010 analyzed 5 morphometry features only on M1 segments of the MCA and A1 segment of the ACA from a set of 115 patients aged from 12 to 78 years. Bullitt et al., 2010 used in-house software to analyze 100 participants aged from 18 to 74 years for vessel number, vessel radius, and vessel tortuosity in the ACA/MCA/PCA. Using a different tool [Neuron_Morpho plugin (Brown et al., 2005), personal.soton.ac.uk/dales/morpho], Wright et al., 2013 recruited 61 healthy participants with age range of 19–64 years and evaluated overall size, bifurcation, and branch features in 6 main artery regions during aging. Mocco et al., 2014, however, had a comprehensive angiography atlas applied to all the arteries, but the measurement was limited to only the diameter of cerebral aneurysms. In this study, we analyzed 8 features across all segments of the intracranial arteries in 163 participants aged 56–85 years, evaluating comprehensive intracranial vasculature features focusing on an older adult population.

Our findings of reduced total number of branches (average order) and increased average tortuosity through aging are consistent with previous research (Bullitt et al., 2010; Wright et al., 2013). Moreover, we found that the decreasing trend in our older adult cohort differs from the trends previously reported in younger cohorts (61 healthy participants, average age = 31.2 ± 10.7, range = 19–64 years) (Wright et al., 2013). As they acquired images from different parameters (0.62 mm isotropic resolution, echo time/repetition time/flip angle = 4.4 ms/24.0 ms/18°) and used a different artery reconstruction method, only total number of branches were compared with our study. The total number of branches was reported to decrease 0.43 per year increase in age (Wright et al., 2013), but we found the decrease was 1.3 per year in our older adult population, which was significantly steeper (p = 0.016) (Fig. 4). The increasing slope of decreasing number of branches suggests that annualized change may increase with age and thus be higher in the older adult population. Further focused investigation of these physiological alterations in intracranial arteries in this age group is needed. Further investigations applying iCafe to population with much wider range of ages is also needed.

4.3. Limitations and future plans

The TOF angiograms used in this study did not cover the vertex of the head. Therefore, some distal vessels near the vertex may not be included. However, all participants were scanned with the same protocol and superior-inferior field of view. A related limitation is that we did not align the vasculatures of participants to each other.

Table 4
Associations between age and the vascular features of the ACA, MCA, and PCA separately

Variable	ACA			MCA			PCA			Difference
	Partial r[a]	(95% CI)	p-value	Partial r[a]	(95% CI)	p-value	Partial r[a]	(95% CI)	p-value	p-value
Total length	−0.17	(−0.32, −0.00)	0.032	−0.08	(−0.21, 0.06)	0.32	−0.26	(−0.38, −0.13)	0.001[b]	0.13
Average diameter	0.07	(−0.09, 0.22)	0.40	0.02	(−0.13, 0.17)	0.82	0.13	(−0.01, 0.27)	0.089	0.84
Volume	−0.11	(−0.26, 0.04)	0.15	−0.04	(−0.18, 0.10)	0.57	−0.17	(−0.30, −0.04)	0.028	0.54
Number of branches	−0.26	(−0.40, −0.09)	0.001[b]	−0.29	(−0.41, −0.17)	<0.001[b]	−0.32	(−0.43, −0.19)	<0.001[b]	>0.99
Average order	−0.29	(−0.43, −0.13)	<0.001[b]	−0.27	(−0.40, −0.14)	<0.001[b]	−0.29	(−0.42, −0.16)	<0.001[b]	>0.99
Average tortuosity	0.02	(−0.11, 0.15)	0.82	0.30	(0.16, 0.42)	<0.001[b]	−0.02	(−0.15, 0.11)	0.80	<0.001[b]
Average bifurcation angle	−0.07	(−0.21, 0.07)	0.39	−0.05	(−0.21, 0.11)	0.53	0.02	(−0.15, 0.18)	0.79	>0.99
Average normalized intensity	0.06	(−0.11, 0.22)	0.48	0.00	(−0.15, 0.15)	0.98	0.13	(−0.01, 0.27)	0.088	0.24

Number of branches and average order of proximal arteries were not included as these are generally fixed values by definition.
Key: ACA, anterior cerebral artery; MCA, middle cerebral artery; PCA, posterior cerebral artery.
[a] Partial Pearson correlation coefficient between the iCafe variable and age, adjusted for sex.
[b] Statistically significant after accounting for the number of comparisons (Holm's method).

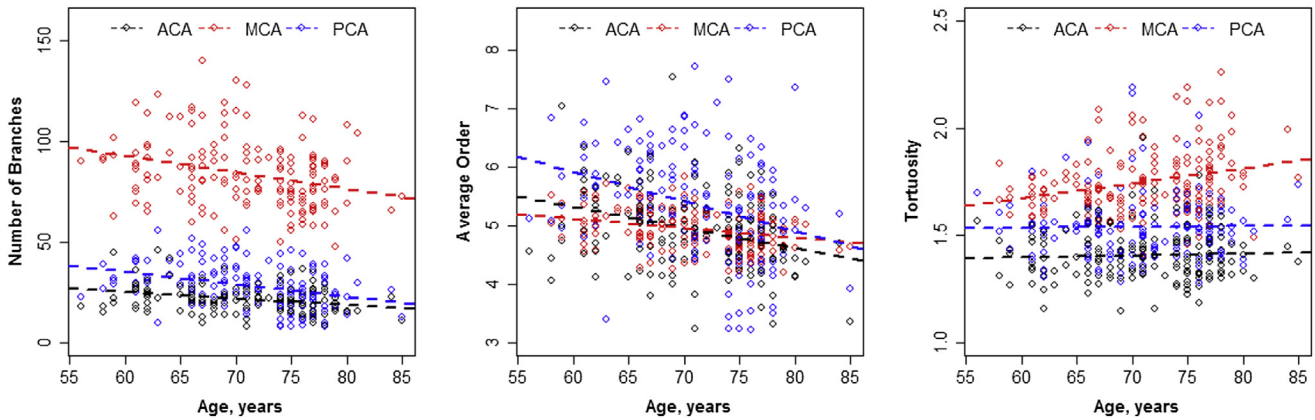

Fig. 3. Scatterplots of selected vascular features of the ACA (black), MCA (red), and PCA territories (blue) versus age. The least squares fits are indicated with the dashed lines. As summarized in Table 3, number of branches and average order of each territory were similarly significantly associated with age. However, tortuosity of the MCA was significantly more correlated with age than tortuosity of the other territories. Abbreviations: ACA, anterior cerebral artery; MCA, middle cerebral artery; PCA, posterior cerebral artery. (For interpretation of the references to color in this figure legend, the reader is referred to the Web version of this article.)

Thus, some individuals with smaller superior-inferior head size may have more arteries included. However, we do not expect this to affect the primary results. In the future, an MRA data set comprising whole-brain vascular region is needed. Full head coverage is likely to further improve the scan-rescan reproducibility of iCafe measurements.

This is a cross-sectional study, so actual within-participant changes of the vascular features with increase in age cannot be assessed. Longitudinal studies with serial imaging data are warranted in the future to corroborate the observations in this study. As TOF MRA is a commonly available, noninvasive technique, such studies are quite feasible in broad populations.

The results may not be generalized to a general population of older adults. First, participants were recruited from a single community in China. Second, while participants had no recent cardiovascular symptoms, carotid artery atherosclerotic plaques were prevalent (62.1%) and a substantial number of high-risk plaques (12.1%) were found in this cohort (Cai et al., 2017).

As the parent study was focused on cardiovascular disease, no measures of cognitive function were collected, precluding an evaluation on the relationship between intracranial artery features and cognitive impairment. Thus, whether changes in intracranial artery features by iCafe lead to cognitive function decline or vice versa will need to be evaluated in future studies. This is a particularly relevant question, given increasing interest in understanding novel mechanisms underlying vascular contributions to dementia (Sweeney et al., 2019).

Processing more participants from multiple sites with a broader range in age using iCafe would facilitate a large database of intracranial vasculature maps. With the help of big data and machine learning, vascular features extracted from the map can be used to develop a brain vascular score, when correlated and validated with participants' clinical information. This brain vascular score could be used along with other well-established brain functional measurements to assess the healthy and diseased brain aging processes.

Finally, a human operator was needed in this study to supervise and correct artery tracings and landmarks automatically processed by iCafe before measurement. As smaller arteries are likely to have weaker flow signal and complex individual variations in brain vasculatures, relatively long processing time (30–60 minutes per participant) was required for manual review to ensure high artery reconstruction quality. However, in future technical developments, these manual artery traces after corrections might be valuable as training samples for machine-learning enhancements to this tool.

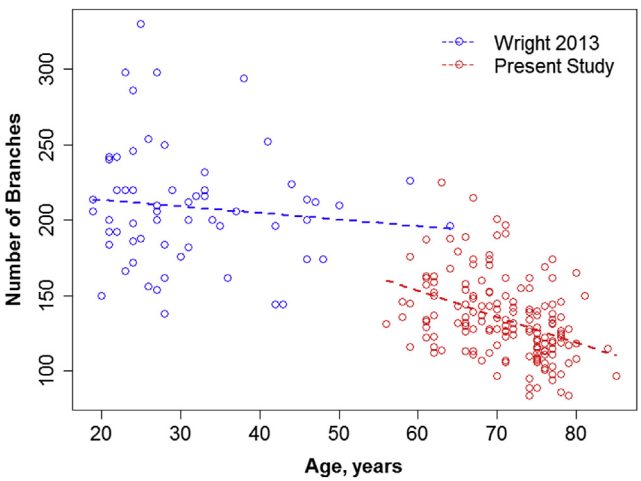

Fig. 4. Relationship between total number of branches and age in the present study and the previous study by Wright et al., 2013. The least squares fits are indicated with the dashed lines.

5. Conclusion

Using the intracranial artery feature extraction technique (iCafe), we found that older age was associated with reduced visibility of vascularity of distal arteries as reflected by quantitative measurements of the number of branches, average artery order, and average tortuosity in a large cohort of older adults. iCafe is a novel postprocessing approach for analyzing cerebral vascular health and may provide useful insights for further research on structural and flow-related changes with aging or other diseases.

Disclosure

The authors have no conflicts of interest to disclose.

Acknowledgements

This research is supported by grants from the National Institutes of Health (R01-NS083503, R01-NS092207, R01-HL103609), National Natural Science Foundation of China (81771825), and Philips Healthcare.

References

Arvanitakis, Z., Capuano, A.W., Leurgans, S.E., Bennett, D.A., Schneider, J.A., 2016. Relation of cerebral vessel disease to Alzheimer's disease dementia and cognitive function in elderly people: a cross-sectional study. Lancet Neurol. 15, 934–943.

Bernier, M., Cunnane, S.C., Whittingstall, K., 2018. The morphology of the human cerebrovascular system. Hum. Brain Mapp. 39, 4962–4975.

Brown, K.M., Donohue, D.E., D'Alessandro, G., Ascoli, G.A., 2005. A cross-platform freeware tool for digital reconstruction of neuronal arborizations from image stacks. Neuroinformatics 3, 343–360.

Brown, W.R., Thore, C.R., 2011. Review: cerebral microvascular pathology in ageing and neurodegeneration. Neuropathol. Appl. Neurobiol. 37, 56–74.

Bullitt, E., Gerig, G., Pizer, S.M., Lin, W., Aylward, S.R., 2003. Measuring tortuosity of the intracerebral vasculature from MRA images. IEEE Trans. Med. Imaging 22, 1163–1171.

Bullitt, E., Rahman, F.N., Smith, J.K., Kim, E., Zeng, D., Katz, L.M., Marks, B.L., 2009. The effect of exercise on the cerebral vasculature of healthy aged subjects as visualized by MR angiography. Am. J. Neuroradiol. 30, 1857–1863.

Bullitt, E., Zeng, D., Mortamet, B., Ghosh, A., Aylward, S.R., Lin, W., Marks, B.L., Smith, K., 2010. The effects of healthy aging on intracerebral blood vessels visualized by magnetic resonance angiography. Neurobiol. Aging 31, 290–300.

Cai, Y., He, L., Yuan, C., Chen, H., Zhang, Q., Li, R., Li, C., Zhao, X., 2017. Atherosclerotic plaque features and distribution in bilateral carotid arteries of asymptomatic elderly population: a 3D multicontrast MR vessel wall imaging study. Eur. J. Radiol. 96, 6–11.

Chen, L., Mossa-Basha, M., Balu, N., Canton, G., Sun, J., Pimentel, K., Hatsukami, T.S., Hwang, J.N., Yuan, C., 2018a. Development of a quantitative intracranial vascular features extraction tool on 3D MRA using semiautomated open-curve active contour vessel tracing. Magn. Reson. Med. 79, 3229–3238.

Chen, L., Mossa-Basha, M., Sun, J., Hippe, D.S., Balu, N., Yuan, Q., Pimentel, K., Hatsukami, T.S., Hwang, J.-N., Yuan, C., 2018b. Quantification of morphometry and intensity features of intracranial arteries from 3D TOF MRA using the intracranial artery feature extraction (iCafe): a reproducibility study. Magn. Reson. Imaging 57, 293–302.

Chen, L., Xie, Y., Sun, J., Balu, N., Mossa-Basha, M., Pimentel, K., Hatsukami, T.S., Hwang, J.N., Yuan, C., 2017a. 3D intracranial artery segmentation using a convolutional autoencoder. Proceedings (IEEE Int. Conf. Bioinformatics Biomed.) 714–717.

Chen, L., Xie, Y., Sun, J., Balu, N., Mossa-Basha, M., Pimentel, K., Hatsukami, T.S., Hwang, J.N., Yuan, C., 2017b. Y-net: 3D intracranial artery segmentation using a convolutional autoencoder. ArXiv arXi2v:1712.07194 [eess.IV].

Farkas, E., de Vos, R.A.I., Donka, G., Jansen Steur, E.N., Mihály, A., Luiten, P.G.M., 2006. Age-related microvascular degeneration in the human cerebral periventricular white matter. Acta Neuropathol. 111, 150–157.

Gutierrez, J., Honig, L., Elkind, M.S.V., Mohr, J.P., Goldman, J., Dwork, A.J., Morgello, S., Marshall, R.S., 2016. Brain arterial aging and its relationship to Alzheimer dementia. Neurology 86, 1507–1515.

Han, Y., Guan, M., Zhu, Z., Li, D., Chen, H., Yuan, C., Li, C., 2018. Assessment of longitudinal distribution of subclinical atherosclerosis in femoral arteries by three-dimensional cardiovascular magnetic resonance vessel wall imaging. J. Cardiovasc. Magn. Reson. 20, 60.

Huang, C., He, Q., Huang, M., Huang, L., Zhao, X., Yuan, C., Luo, J., 2017a. Non-invasive identification of vulnerable atherosclerotic plaques using texture analysis in ultrasound carotid elastography: an in vivo feasibility study validated by magnetic resonance imaging. Ultrasound Med. Biol. 43, 817–830.

Huang, C., Pan, X., He, Q., Huang, M., Huang, L., Zhao, X., Yuan, C., Bai, J., Luo, J., 2016. Ultrasound-Based carotid elastography for detection of vulnerable atherosclerotic plaques validated by magnetic resonance imaging. Ultrasound Med. Biol. 42, 365–377.

Huang, M., Hippe, D.S., Huang, L., Zhao, X., Luo, J., Zeng, Q., Yuan, C., 2017b. A noninvasive sonographic study of multisite atherosclerosis in an elderly Chinese population. J. Ultrasound Med. 36, 639–647.

Jiang, L., Chen, H., Li, R., Han, X., Chen, Z., He, L., Yuan, C., Zhao, X., 2015. Associations of arterial distensibility between carotid arteries and abdominal aorta by MR. J. Magn. Reson. Imaging 41, 1138–1142.

Kalaria, R.N., 1996. Cerebral vessels in ageing and Alzheimer's disease. Pharmacol. Ther. 72, 193–214.

Kamenskiy, A.V., Pipinos, I.I., Carson, J.S., MacTaggart, J.N., Baxter, B.T., 2015. Age and disease-related geometric and structural remodeling of the carotid artery. J. Vasc. Surg. 62, 1521–1528.

Kety, S., 1955. Human Blood flow and oxygen consumption as related to aging. J. Chronic Dis. 3, 478–486.

Lakatta, E.G., Levy, D., 2003. Arterial and cardiac aging: major shareholders in cardiovascular disease enterprises: part I: aging arteries: a "set up" for vascular disease. Circulation 107, 139–146.

Mocco, J., Huston, J., Fargen, K.M., Torner, J., Brown, R.D., 2014. An angiographic atlas of intracranial arterial diameters associated with cerebral aneurysms. J. Neurointerv. Surg. 6, 533–535.

Najjar, S.S., Scuteri, A., Lakatta, E.G., 2005. Arterial aging: is it an immutable cardiovascular risk factor? Hypertension 46, 454–462.

Nyul, L.G., Udupa, J.K., Zhang, X., 2000. New variants of a method of MRI scale standardization. IEEE Trans. Med. Imaging 19, 143–150.

Qiao, H., He, Q., Chen, Z., Xu, D., Huang, L., He, L., Jiang, L., Li, R., Luo, J., Yuan, C., Zhao, X., 2016. Identification of early atherosclerotic lesions in carotid arteries with quantitative characteristics measured by 3D MRI. J. Magn. Reson. Imaging 44, 1270–1276.

Raz, N., Lindenberger, U., Rodrigue, K.M., Kennedy, K.M., Head, D., Williamson, A., Dahle, C., Gerstorf, D., Acker, J.D., 2005. Regional brain changes in aging healthy adults: general trends, individual differences and modifiers. Cereb. Cortex 15, 1676–1689.

Riddle, D.R., Sonntag, W.E., Lichtenwalner, R.J., 2003. Microvascular plasticity in aging. Ageing Res. Rev. 2, 149–168.

Scahill, R.I., Frost, C., Jenkins, R., Whitwell, J.L., Rossor, M.N., Fox, N.C., 2003. A longitudinal study of brain volume changes in normal aging using serial registered magnetic resonance imaging. Arch. Neurol. 60, 989.

Scheinberg, P., Blackburn, I., Rich, M., Saslaw, M., 1953. Effects of aging on cerebral circulation and metabolism. AMA Arch. Neurol. Psychiatry 70, 77–85.

Sweeney, M.D., Montagne, A., Sagare, A.P., Nation, D.A., Schneider, L.S., Chui, H.C., Harrington, M.G., Pa, J., Law, M., Wang, D.J.J., Jacobs, R.E., Doubal, F.N., Ramirez, J., Black, S.E., Nedergaard, M., Benveniste, H., Dichgans, M., Iadecola, C., Love, S., Bath, P.M., Markus, H.S., Salman, R.A., Allan, S.M., Quinn, T.J., Kalaria, R.N., Werring, D.J., Carare, R.O., Touyz, R.M., Williams, S.C.R., Moskowitz, M.A., Katusic, Z.S., Lutz, S.E., Lazarov, O., Minshall, R.D., Rehman, J., Davis, T.P., Wellington, C.L., González, H.M., Yuan, C., Lockhart, S.N., Hughes, T.M., Chen, C.L.H., Sachdev, P., O'Brien, J.T., Skoog, I., Pantoni, L., Gustafson, D.R., Biessels, G.J., Wallin, A., Smith, E.E., Mok, V., Wong, A., Passmore, P., Barkof, F., Muller, M., Breteler, M.M.B., Román, G.C., Hamel, E., Seshadri, S., Gottesman, R.F., van Buchem, M.A., Arvanitakis, Z., Schneider, J.A., Drewes, L.R., Hachinski, V., Finch, C.E., Toga, A.W., Wardlaw, J.M., Zlokovic, B.V., 2019. Vascular dysfunction—the disregarded partner of Alzheimer's disease. Alzheimer's Dement. 15, 158–167.

Ungvari, Z., Kaley, G., De Cabo, R., Sonntag, W.E., Csiszar, A., 2010. Mechanisms of vascular aging: new perspectives. J. Gerontol. A. Biol. Sci. Med. Sci. 65 A, 1028–1041.

Viviani, R., 2016. A digital atlas of middle to large brain vessels and their relation to cortical and subcortical structures. Front Neuroanat. 10, 1–9.

Wang, Y., Narayanaswamy, A., Tsai, C.L., Roysam, B., 2011. A broadly applicable 3-D neuron tracing method based on open-curve snake. Neuroinformatics 9, 193–217.

Webster, M.W., Makaroun, M.S., Steed, D.L., Smith, H.A., Johnson, D.W., Yonas, H., 1995. Compromised cerebral blood flow reactivity is a predictor of stroke in patients with symptomatic carotid artery occlusive disease. J. Vasc. Surg. 21, 338–344.

Wright, S.N., Kochunov, P., Mut, F., Bergamino, M., Brown, K.M., Mazziotta, J.C., Toga, A.W., Cebral, J.R., Ascoli, G.A., 2013. Digital reconstruction and morphometric analysis of human brain arterial vasculature from magnetic resonance angiography. Neuroimage 82, 170–181.

Yonas, H., Smith, H.A., Durham, S.R., Pentheny, S.L., Johnson, D.W., 1993. Increased stroke risk predicted by compromised cerebral blood flow reactivity. J. Neurosurg. 79, 483–489.

Zhou, C., Qiao, H., He, L., Yuan, C., Chen, H., Zhang, Q., Li, R., Wang, W., Du, F., Li, C., Zhao, X., 2016. Characterization of atherosclerotic disease in thoracic aorta: a 3D, multicontrast vessel wall imaging study. Eur. J. Radiol. 85, 2030–2035.

Zurada, A., Gielecki, J., Tubbs, R.S., Loukas, M., Maksymowicz, W., Cohen-Gadol, A.A., Michalak, M., Chlebiej, M., Zurada-Zielińska, A., 2011. Three-dimensional morphometrical analysis of the M1 segment of the middle cerebral artery: potential clinical and neurosurgical implications. Clin. Anat. 24, 34–46.

Zurada, A., St Gielecki, J., Tubbs, R.S., Loukas, M., Zurada-Zielińska, A., Maksymowicz, W., Nowak, D., Cohen-Gadol, A.A., 2010. Three-dmensional morphometry of the A1 segment of the anterior cerebral artery with neurosurgical relevance. Neurosurgery 67, 1768–1782.